



Full length article

Synthesis and evaluation of the anticancer activity of bischalcone analogs in human lung carcinoma (A549) cell line

Jie Yang^{**}, Wen-Wen Mu, Guo-Yun Liu^{*}

School of Pharmacy, Liaocheng University, 1 Hunan Street, Liaocheng, Shandong, 252000, China



ARTICLE INFO

Keywords:

Bischalcone
Curcumin analogs
Reactive oxygen species
Apoptosis
Human lung carcinoma (A549) cell line
Bax

ABSTRACT

Bischalcone has gained much attention because of its wide range of application in pharmaceutical chemistry. This work aims to evaluate the antiproliferation effects and explore the anticancer mechanism of bischalcone analogs on human lung cancer A549 cells. In this study, we synthesized a series of bischalcone analogs via Aldol condensation reaction; MTT method was used to evaluate the antiproliferation effects; the 2',7'-dichloro-fluorescein fluorescence assay was used to determine the intracellular reactive oxygen species levels; the glutathione reductase-DTNB recycling assay was used to detect the redox imbalance; determination of thio-barbituric acid-reactive substance was used to evaluate the lipid peroxidation; Rhodamine 123 was used to test the mitochondrial membrane potential (MMP); the FITC/PI kit was used to detect the apoptosis; Western blotting was used to detect the expression of Bax and Caspase 3. After treatment with curcumin and bischalcone analogs, compounds **1d** and **1g**, the more stabilities compounds than curcumin, exhibited much higher potency in A549 cells than curcumin and other bischalcone analogs. Further mechanism of action studies revealed that **1d** and **1g** exhibited more stronger reactive oxygen species production abilities than curcumin and accompanied by the redox imbalance, lipid peroxidation, the loss of MMP, the activation of Bax and Caspase 3, and ultimately resulted in apoptosis of A549 cell. These data suggest that enhancing the reactive oxygen species generation ability of bischalcone analogs may be a promising strategy for the treatment of human lung cancer.

1. Introduction

Lung cancer is one of the most devastating cancers with high morbidity and mortality in the worldwide (Malvezzi et al., 2019). The mortality rate for lung cancer will increase in the world, especially in women by 40% in 2030 (<https://pubmed.ncbi.nlm.nih.gov/?term=Martin%20et%20al%202018>). The common strategies, containing surgery, chemotherapy, radiotherapy and targeted therapy, are used to treat the lung cancer. While the side-effects of gastrointestinal response and renal dysfunction have been reported to be associated with chemotherapy (<https://pubmed.ncbi.nlm.nih.gov/?term=Li%20et%20al%202019>). Therefore, it is essential to search for new anticancer agents to treat lung cancer.

Natural products and their derivatives have contributed significantly to drug discovery, especially in the development of anticancer drugs (<https://pubmed.ncbi.nlm.nih.gov/?term=Reddy%20et%20al%202012>).

One of the simplest natural compounds is chalcone, a curcumin analog and it is a bioactive component of many edible plants (<https://pubmed.ncbi.nlm.nih.gov/?term=Wang%20et%20al%202019>). Chalcone, bearing an α,β -unsaturated carbonyl moiety, has been shown to be a potential chemopreventive and anticancer agents (<https://pubmed.ncbi.nlm.nih.gov/?term=Wang%20et%20al%202019>). Chalcone could enhance intracellular reactive oxygen species levels in human liver hepatocellular carcinoma (HepG2) cells. The bischalcone, containing two chalcone units in a single structure, also exhibits spectral biological activity including anti-inflammatory and anticancer activity (<https://pubmed.ncbi.nlm.nih.gov/?term=Reddy%20et%20al%202012>). Similar compounds featuring two α,β -unsaturated carbonyl units have been described in the literature, while information of their anticancer activity and mechanism against lung cancer is relatively inadequate.

* Corresponding author.

** Corresponding author.

E-mail address: guoyunliu@126.com (J. Yang).<https://doi.org/10.1016/j.ejphar.2020.173396>

Received 7 June 2020; Received in revised form 17 July 2020; Accepted 22 July 2020

Available online 14 August 2020

0014-2999/© 2020 Elsevier B.V. All rights reserved.

In this study, a series of bischalcone analogs are synthesized according to the Aldol condensation protocol (Scheme 1). Thus we focus on the cytotoxicity and explore the anticancer mechanism against human lung cancer A549 cells.

2. Materials and methods

2.1. Materials

Roswell Park Memorial Institute (RPMI)-1640 was from Hyclone. 3-(4,5-dimethylthiazol-2-yl)-2,5-diphenyltetrazolium bromide (MTT), rhodamine 123, 2',7'-dichlorofluorescein diacetate, the reduced (GSH) and oxidized (GSSG) glutathione, 2-vinylpyridine (97%) and thio-barbituric acid were obtained from Beyotime. Radio Immunoprecipitation Assay (RIPA) buffer, 50°C Cooktail proteinase inhibitor, GAPDH, the primary antibodies and HRP-labeled secondary antibodies were purchased from Servicebio. Annexin V-FITC/PI apoptosis detection kit was purchased from BD Biosciences. Substituted acetophenone, 1,4-phthalaldehyde and curcumin were from EnergyChemical. All other chemicals were of the highest quality available.

2.2. Synthesis of the curcumin analogs

2.2.1. General procedure for the synthesis of 1a-1i

The bischalcone analogs were synthesized according to the published procedure (https://pubmed.ncbi.nlm.nih.gov/?term=Mart%C3%ADn-S%C3%A1nchez+JC&cauthor_id=30068667 Winter et al., 2014). Briefly, aqueous NaOH (60%, w/v, 8 ml) was added dropwise to a vigorously stirred solution of 1,4-phthalaldehyde (5 mmol) and relevant acetophenone (10 mmol) in ethanol (20 ml) at 0 °C. After 24 h stirring at room temperature, distilled water and 10% hydrochloric acid solution were added for total precipitation of the compounds. Then the crude products were purified with a silica gel column. Their structures were confirmed by ¹H and ¹³C NMR spectroscopy.

(2*E*, 2'*E*)-3,3'-(1,4-phenylene)bis(1-(2-hydroxyphenyl)prop-2-en-1-one) (1a). Yield: 44.2%; Yellow solid; m.p.: 228-231 °C, ¹H NMR (400 MHz, *d*₆-DMSO), δ 12.48 (s, 2H), 8.30 (dd, *J* = 8.0, 1.6 Hz, 2H), 8.17 (d, *J* = 16 Hz, 2H), 8.03 (d, *J* = 8.0 Hz, 4H), 7.90 (d, *J* = 16 Hz, 2H), 7.61-7.57 (m, 2H), 7.05-7.03 (m, 4H); ¹³C NMR (100 MHz, CDCl₃), δ 193.9, 162.2, 144.0, 137.1, 136.8, 131.4, 130.1, 123.6, 121.4, 119.6, 118.2.

(2*E*, 2'*E*)-3,3'-(1,4-phenylene)bis(1-(3-hydroxyphenyl)prop-2-en-1-one) (1b). Yield: 51.6%, light yellow solid; m.p.: 244-246 °C, ¹H NMR (400 MHz, *d*₆-DMSO), δ 9.83 (s, 2H), 7.98-7.94 (m, 6H), 7.77 (d, *J* = 16 Hz, 2H), 7.68 (d, *J* = 8.0 Hz, 2H), 7.48 (s, 2H), 7.41 (t, *J* = 8.0 Hz, 2H), 7.09 (dd, *J* = 8.0, 2.4 Hz, 2H); ¹³C NMR (100 MHz, CDCl₃), δ 189.5, 158.2, 143.3, 139.4, 137.1, 130.3, 129.8, 123.6, 120.8, 120.1, 115.1.

(2*E*, 2'*E*)-3,3'-(1,4-phenylene)bis(1-(4-hydroxyphenyl)prop-2-en-1-one) (1c). Yield: 55.8%, yellow powder; mp 219-222 °C; ¹H NMR (300

MHz, (CD₃)₂CO), δ 8.12 (d, *J* = 9.0 Hz, 4H), 7.97 (d, *J* = 15.9 Hz, 2H), 7.92 (s, 4H), 7.77 (d, *J* = 15.9 Hz, 2H), 6.99 (d, *J* = 9.0 Hz, 4H); ¹³C NMR (75 MHz, CDCl₃), δ 187.0, 162.2, 157.8, 141.8, 136.6, 131.2, 129.1, 123.0, 115.4.

(2*E*, 2'*E*)-3,3'-(1,4-phenylene)bis(1-(2-methoxyphenyl)prop-2-en-1-one) (1d). Yield: 42.5%, light yellow solid; mp 150-152 °C, ¹H NMR (400 MHz, CDCl₃), δ 7.65-7.60 (m, 8H), 7.51-7.47 (m, 2H), 7.45 (d, *J* = 16 Hz, 2H), 7.07 (t, *J* = 8.0 Hz, 2H), 7.02 (d, *J* = 8.0, 2.4 Hz, 2H), 3.92 (s, 6H); ¹³C NMR (100 MHz, CDCl₃), δ 192.6, 158.2, 141.9, 136.9, 133.1, 130.4, 129.1, 128.8, 127.8, 120.8, 111.6, 55.8, 55.7.

(2*E*, 2'*E*)-3,3'-(1,4-phenylene)bis(1-(3-methoxyphenyl)prop-2-en-1-one) (1e). Yield: 50.6%, yellow powder; mp 180-182 °C, ¹H NMR (400 MHz, CDCl₃), δ 7.84 (d, *J* = 16 Hz, 2H), 7.70 (s, 4H), 7.63-7.55 (m, 6H), 7.45 (t, *J* = 8.0 Hz, 2H), 7.17 (dd, *J* = 8.0, 2.4 Hz, 2H), 3.90 (s, 6H); ¹³C NMR (100 MHz, CDCl₃), δ 189.9, 159.9, 143.5, 139.4, 136.9, 129.6, 129.0, 123.1, 121.1, 119.4, 112.9, 55.5.

(2*E*, 2'*E*)-3,3'-(1,4-phenylene)bis(1-(4-methoxyphenyl)prop-2-en-1-one) (1f). Yield: 55.8%, yellow powder; mp 245-248 °C; ¹H NMR (300 MHz, CDCl₃), δ 8.05 (d, *J* = 8.4 Hz, 4H), 7.80 (d, *J* = 15.9 Hz, 2H), 7.68 (s, 4H), 7.59 (d, *J* = 15.9 Hz, 2H), 7.00 (d, *J* = 8.4 Hz, 4H), 3.90 (s, 6H); ¹³C NMR (75 MHz, CDCl₃), δ 188.4, 163.5, 142.7, 136.9, 130.9, 130.8, 128.8, 122.8, 114.0, 113.9, 55.5.

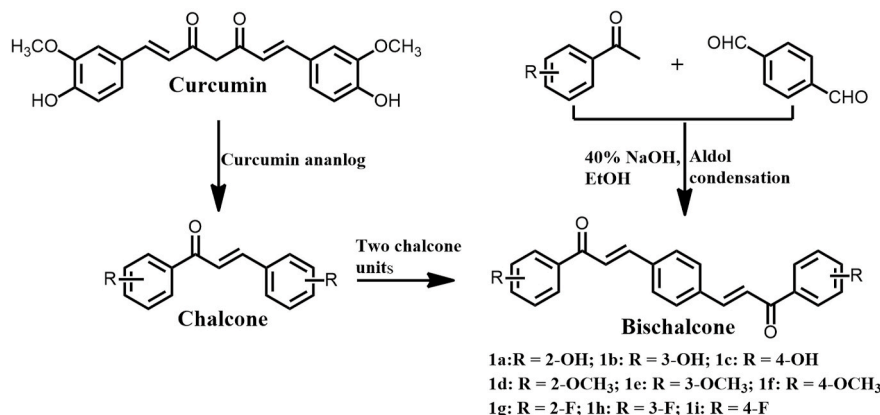
(2*E*, 2'*E*)-3,3'-(1,4-phenylene)bis(1-(2-fluorophenyl)prop-2-en-1-one) (1g). Yield: 56.2%, yellow powder; mp 135-138 °C; ¹H NMR (500 MHz, CDCl₃), δ 7.82 (t, *J* = 8.0 Hz, 2H), 7.73 (d, *J* = 16.0 Hz, 2H), 7.67 (s, 4H), 7.53-7.56 (m, 2H), 7.44 (d, *J* = 16.0 Hz, 2H); 7.26 (d, *J* = 8.0 Hz, 2H); 7.17 (t, *J* = 8.0 Hz, 2H).

(2*E*, 2'*E*)-3,3'-(1,4-phenylene)bis(1-(3-fluorophenyl)prop-2-en-1-one) (1h). Yield: 61.5%, yellow powder; mp 141-144 °C; ¹H NMR (500 MHz, CDCl₃), δ 8.07-8.10 (m, 4H), 7.81 (d, *J* = 16.0 Hz, 2H), 7.71 (s, 4H), 7.55 (d, *J* = 16.0 Hz, 2H); 7.18 (d, *J* = 8.0 Hz, 4H).

(2*E*, 2'*E*)-3,3'-(1,4-phenylene)bis(1-(4-fluorophenyl)prop-2-en-1-one) (1i). Yield: 63.8%, yellow powder; mp 235-237 °C; ¹H NMR (500 MHz, CDCl₃), δ 8.06 (dd, *J* = 8.0 Hz, 4H), 7.81 (d, *J* = 16.0 Hz, 2H), 7.70 (s, 4H), 7.55 (d, *J* = 16.0 Hz, 2H), 7.18 (d, *J* = 8.0 Hz, 4H).

2.3. MTT assay

Human lung carcinoma cells (A549) were from the Shanghai Institute of Biochemistry and Cell Biology, Chinese Academy of Sciences. Cells were cultured with RPMI-1640 medium at 37 °C in a humidified atmosphere with 5% CO₂. A549 cells were seeded in 96-well plates at a density of 3 × 10³/well and incubated for 24 h. Then the cells were treated for another 48 h with compounds at the selected concentration. The next steps were processed according to the reported reference (https://pubmed.ncbi.nlm.nih.gov/?term=Mart%C3%ADn-S%C3%A1nchez+JC&cauthor_id=30068667



Scheme 1. Molecular structures and synthetic routes of bischalcone analogs.

https://pubmed.ncbi.nlm.nih.gov/?term=Mart%C3%ADn-S%C3%A1nchez+JC&cauthor_id=30068667Liu+et+al.,+2016).

2.4. Stability assay

Stability of curcumin and bischalcone analogs was monitored as described previously (https://pubmed.ncbi.nlm.nih.gov/?term=Mart%C3%ADn-S%C3%A1nchez+JC&cauthor_id=30068667Liu+et+al.,+2016). Briefly, curcumin or bischalcone analogs (**1d** and **1g**) was dissolved in RPMI 1640 supplemented with 10% (v/v) heat-inactivated fetal calf serum, then their maximum absorbance were monitored by using a micro-plate reader for 120 min at 10-min intervals.

2.5. Cell apoptosis analysis

The apoptosis induction activity of curcumin and **1d** were detected as previously described (https://pubmed.ncbi.nlm.nih.gov/?term=Mart%C3%ADn-S%C3%A1nchez+JC&cauthor_id=30068667Liu+et+al.,+2016). 3×10^5 A549 cells were treated with the tested compounds in 6-well plates for 24 h. After that, the cells were collected and determined by FITC/PI kit using a flow cytometry.

2.6. Intracellular reactive oxygen species measurement

The 2',7'-dichlorofluorescein fluorescence assay was used to determine the intracellular reactive oxygen species levels as described previously (https://pubmed.ncbi.nlm.nih.gov/?term=Mart%C3%ADn-S%C3%A1nchez+JC&cauthor_id=30068667Liu+et+al.,+2018). 3×10^5 A549 cells were treated with the tested compounds in 6-well plates for 6 h. Next, the harvested cells were incubated with 3 μ M DCFH-DA for 30 min at 37 °C and analyzed immediately by flow cytometry.

2.7. Measurement of GSH and GSSG levels

A549 (3×10^5 cells/well) cells were seeded in 6-well plates in growth medium and treated with the tested compound for 6 h. Intracellular GSH and GSSG contents were performed by the glutathione reductase-DTNB recycling assay as described previously (https://pubmed.ncbi.nlm.nih.gov/?term=Mart%C3%ADn-S%C3%A1nchez+JC&cauthor_id=30068667Zhang+et+al.,+2018).

2.8. Determination of thiobarbituric acid-reactive substance (TBARS)

3×10^5 A549 cells were incubated with the tested compound for 18 h in 6-well plates. Then, the cells were harvested and lysed. Lipid peroxidation was determined by the protocol as previously described (https://pubmed.ncbi.nlm.nih.gov/?term=Mart%C3%ADn-S%C3%A1nchez+JC&cauthor_id=30068667Mu+et+al.,+2020).

2.9. Analysis of mitochondrial membrane potential

3×10^5 A549 cells were treated with the tested compound for 18 h in 6-well plates. Next, the cells were collected and incubated with Rhodamine 123 (5 μ M) for 30 min at 37 °C and analyzed using a flow cytometry as previously described (https://pubmed.ncbi.nlm.nih.gov/?term=Mart%C3%ADn-S%C3%A1nchez+JC&cauthor_id=30068667Yang+et+al.,+2019).

2.10. Western blotting analysis

After treatment with the tested compounds, the expression of Caspase 3 and Bax proteins of A549 cells were analyzed by Western blot as previously described (https://pubmed.ncbi.nlm.nih.gov/?term=Mart%C3%ADn-S%C3%A1nchez+JC&cauthor_id=30068667Ma+et+al.,+2020). Briefly, the harvested A549 cells were lysed with ice-cold RIPA lysis buffer containing proteinase inhibitors, followed by quantification

of the proteins with a Bicinchoninic Acid (BCA) protein assay kit. After separation in the gel and transfer, the polyvinylidene fluoride (PVDF) membranes were blocked and incubated with the primary antibodies before incubation with the corresponding Horseradish Peroxidase (HRP)-labeled secondary antibody. Subsequently, the blots were washed and visualized by the enhanced chemiluminescence (ECL) detection.

2.11. Statistical analysis

The data are expressed as the mean \pm S.D. of at least three independent experiments.

Data were analyzed by use of SPSS software 17.0 (SPSS, Inc., Chicago, IL, USA). The difference between two groups was analyzed by one-way analysis of variance (ANOVA) followed by Dunnett test (compare all drug treatment groups vs. control). The values were considered significant at $P < 0.05$. *: $P < 0.05$; **: $P < 0.01$; ***: $P < 0.001$ compared with control.

3. Results

3.1. Synthesis

Compounds proposed in this work were synthesized according to previously described procedure (https://pubmed.ncbi.nlm.nih.gov/?term=Mart%C3%ADn-S%C3%A1nchez+JC&cauthor_id=30068667Winter+et+al.,+2014) (Scheme 1). **1a-1i** were synthesized via Aldol condensation from 1,4-phthalaldehyde and relevant acetophenone at moderate yields after purification by silica gel column chromatography. All compounds were characterized by ^1H NMR and ^{13}C NMR.

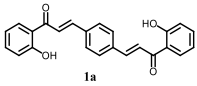
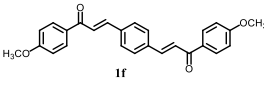
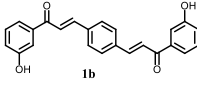
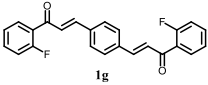
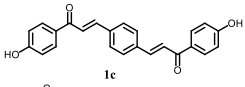
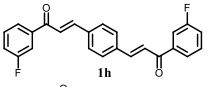
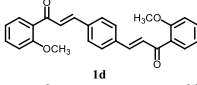
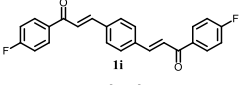
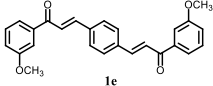
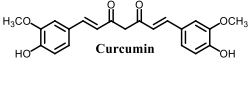
3.2. Antiproliferative activity of bischalcone analogs in vitro

It has been reported that bischalcone showed a spectral anti-cancer properties (https://pubmed.ncbi.nlm.nih.gov/?term=Mart%C3%ADn-S%C3%A1nchez+JC&cauthor_id=30068667Reddy+et+al.,+2012). Therefore, MTT assays were used to evaluate the cytotoxicity of curcumin and bischalcone analogs on A549 cancer cells after a 48 h treatment *in vitro*, and the IC_{50} values are listed in Table 1. Compounds **1d** and **1g** displayed more excellent cytotoxicity than curcumin and other bischalcone analogs. This result may be due to the "ortho effect" of substituents which could enhance the antiproliferation activity of mono-carbonyl curcumin analogs against cancer cells (https://pubmed.ncbi.nlm.nih.gov/?term=Mart%C3%ADn-S%C3%A1nchez+JC&cauthor_id=30068667Liu+et+al.,+2016). Especially, **1d** and **1g** surfaced as potent lead compounds exhibiting about 9-time and 5-time higher potency than curcumin, respectively. This result may be related with the more stabilities of **1d** and **1g** in RPMI 1640 supplemented with 10% (v/v) heat-inactivated fetal calf serum than curcumin (Fig. 1). Therefore, **1d** and **1g** were selected for further underlying their anti-cancer mechanisms on A549 cells.

3.3. Apoptosis induction in A549 cells after treatment with 1d and 1g

Apoptosis, known as type I programmed cell death, is a common cell death pathway in chemotherapeutic agent (https://pubmed.ncbi.nlm.nih.gov/?term=Mart%C3%ADn-S%C3%A1nchez+JC&cauthor_id=30068667Benedetti+et+al.,+2018). To investigate the surveyed reduction in cell viability brought by **1d** and **1g** was rely on induction of apoptosis, an annexinV-FITC/PI double staining was executed and followed by flow cytometry analysis. As shown in Fig. 2, **1d** and **1g** exhibited significant apoptosis of A549 cells in a dose-dependent manner ($P < 0.05$). In particular, treatment with 60 μ M **1d** and 60 μ M **1g**, which exhibited stronger apoptosis inducing activity than 60 μ M curcumin, caused 66.4% and 52.4% late apoptotic cells, respectively. The sequence of apoptotic activity of these compounds was in

Table 1
Cytotoxicity of curcumin and its analogs against A549 cells.

Comps.	IC ₅₀ (μM)	Comps.	IC ₅₀ (μM)
 1a	>200	 1f	>200
 1b	19.2 ± 1.4	 1g	9.7 ± 0.8
 1c	>200	 1h	>200
 1d	5.5 ± 0.7	 1i	>200
 1e	180.7 ± 9.9	 Curcumin	52.3 ± 1.1

The IC₅₀ value is the concentration of a compound tested to cause 50% inhibition of cell viability after 48 h of treatment, and is expressed as the mean ± S.D. for three determinations.

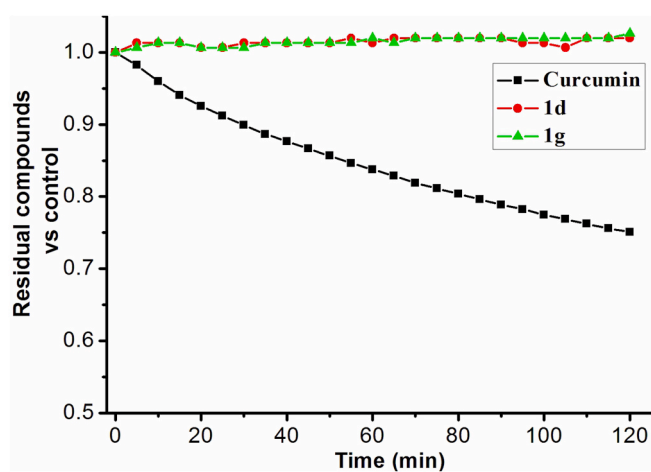


Fig. 1. Stability assessment on curcumin (50 μM), **1d** (50 μM) and **1g** (50 μM) in RPMI 1640 supplemented with 10% (v/v) heat-inactivated fetal calf serum at 25 °C by monitoring the decrease in their maximum absorbance.

accordance with their cytotoxicity in A549 cells, which suggest that the cytotoxicity of the bischalcones was rely on their induction of apoptosis.

3.4. Effects of **1d** and **1g** on the intracellular reactive oxygen species generation

Intracellular reactive oxygen species can modulate cell proliferation, apoptosis and other physiological reactions (https://pubmed.ncbi.nlm.nih.gov/?term=Martin%20et%20al%202019&cauthor_id=30068667Zhang et al., 2019). Therefore, we decided to determined whether **1d** and **1g** could increase reactive oxygen species generation in A549 cells using 2',7'-dichlorofluorescein diacetate. As expected, remarkable increase in the generation of reactive oxygen species was investigated in A549 cells exposed to different concentrations of **1d** and **1g** (15, 30 and 60 μM) relative to that of control ($P < 0.01$, Fig. 3). It was observed that **1d** and **1g** showed an excellent dose-dependent fashion in reactive oxygen species production and exhibited more potent ability than curcumin. Specifically, cells treated with 60 μM **1d** showed a 5-time increase compared to the control ($P < 0.001$, Fig. 3). These results were relationship with the apoptotic activity of these compounds and revealed that reactive oxygen species generation ability is a critical

factor in the apoptosis induced by bischalcones.

3.5. Effects of **1d** and **1g** on the redox balance

Given that intracellular redox imbalance, which was evaluated by the ratio of GSH and its disulfide GSSG, usually occurred when a sustained higher reactive oxygen species production (Diebold). The glutathione reductase-DTNB recycling assay was used to evaluate the ratio of GSH/GSSG of A549 cells after **1d** and **1g** treatment. It was found that **1d** and **1g** sharply decreased the ratio of GSH/GSSG in a dose-dependent manner ($P < 0.05$, Fig. 4). In addition, at a concentration of 60 μM, **1d** caused a 3-fold decline in the ratio of GSH/GSSG relative to the control ($P < 0.001$, Fig. 4), which was in line with its more powerful reactive oxygen species production abilities. These results indicated that the intracellular extensive reactive oxygen species resulted in the redox imbalance of A549 cells.

3.6. Effects of **1d** and **1g** on the lipid peroxidation of A549 cells

The sustained higher reactive oxygen species production of cells also could target to the lipids of the plasma membrane and result in lipid peroxidation (https://pubmed.ncbi.nlm.nih.gov/?term=Martin%20et%20al%202020&cauthor_id=30068667Serrano et al., 2020), which was raised as determination of the amounts of malondialdehyde (MDA). As seen in Fig. 5, exposure of the cells to **1d** and **1g** resulted in a remarkable increase of the levels of MDA and exhibited a prime dose-dependent manner. Additionally, treatment with 60 μM **1d** and 60 μM **1g**, the amounts of MDA with about 2-fold and 1.9-fold increase respectively compared with the control ($P < 0.01$, Fig. 5).

3.7. Effects of **1d** and **1g** on the loss of mitochondrial membrane potential (MMP)

As demonstrated in the literature, the excess production of reactive oxygen species is often accompanied with the disruption of mitochondrial membrane, a critical event in early cell apoptosis (Kroemer). For the sake of investigating whether the disruption of the MMP was related to induction of cell apoptosis, the MMP in A549 cells was determined with Rhodamine 123 by flow cytometry. Fig. 6 shows that **1d** and **1g** caused a significant decrease of MMP in a perfect dose-dependent fashion ($P < 0.01$). Moreover, **1d** and **1g** were more active than the leading curcumin in the loss of MMP. In particular, treatment with 60 μM **1d** and 60 μM **1g** resulted in about 3-time and 2-time decrease of the MMP respectively

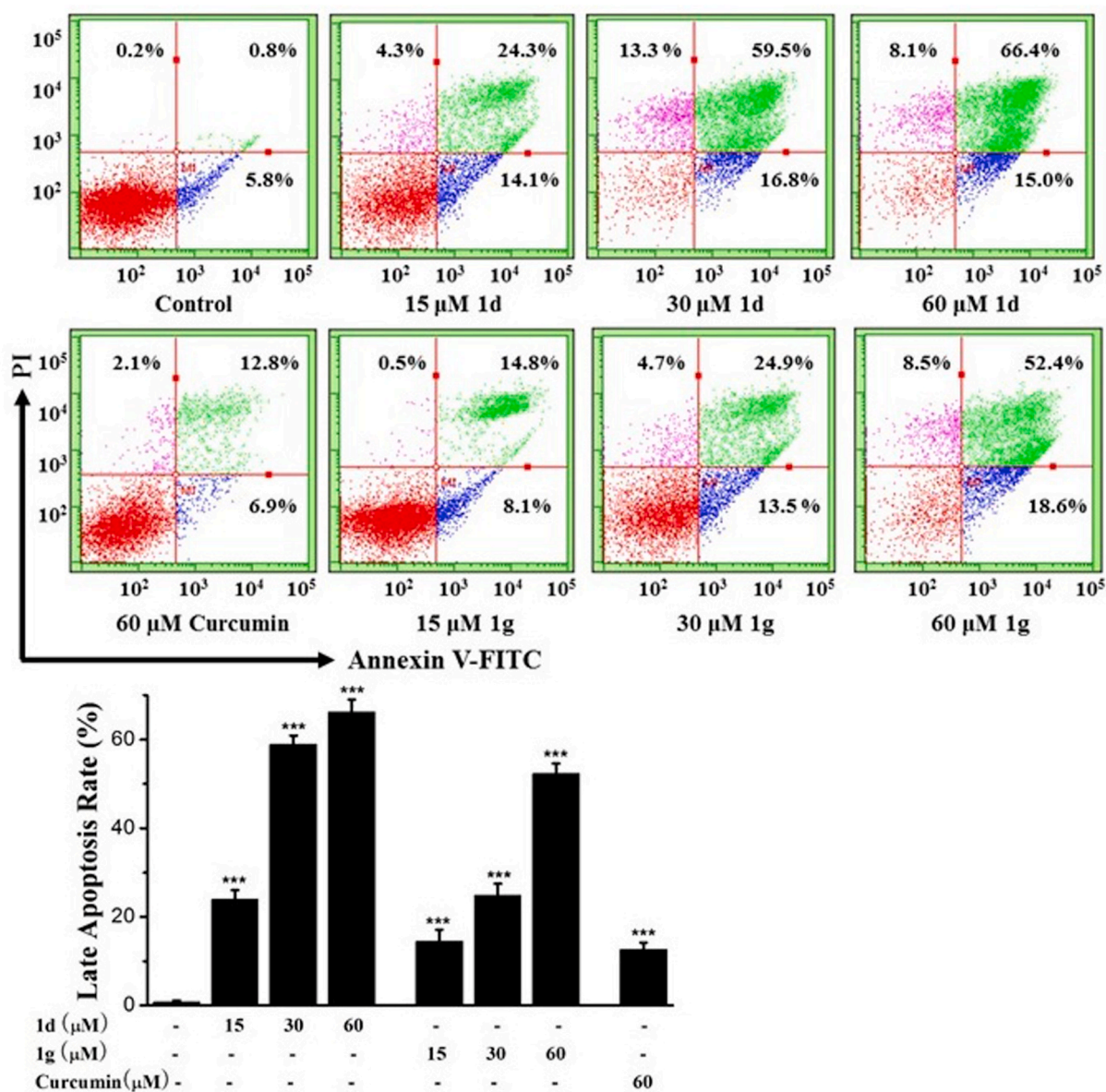


Fig. 2. Flow cytometric analysis for apoptotic induction of A549 cells treated with curcumin and bischalcone analogs (**1d** and **1g**) for 24 h * $P < 0.05$, ** $P < 0.01$, *** $P < 0.001$ compared with control.

relative to the control ($P < 0.001$, Fig. 6). These results were in line with the reactive oxygen species production abilities and apoptosis inducing activities of **1d** and **1g** on A549 cell.

3.8. 1d and 1g promoted the Bax and Caspase 3 expression

Bax and Caspase 3 proteins play integral roles in the initiation and execution of apoptosis (Boice). Therefore, we investigated for the Bax and Caspase 3 activities by western blotting. As expected, both the expression levels of Bax and Caspase 3 proteins were remarkably increased after compounds **1d** and **1g** treatment compared with control (Fig. 7). In particular, compound **1d** could increase the expression of Caspase 3 in a dose-dependent manner, and **1g** enhanced the levels of Bax protein in a dose-dependent fashion. These results indicated that the bischalcone analogs **1d** and **1g** could promote A549 cell apoptosis through activating the expression of Bax and Caspase 3.

4. Discussion

Lung cancer is one of the most common life-threatening malignancies in the worldwide (Malvezzi et al., 2019), accounting for almost 13% of all cancer diagnoses and nearly 19% of total cancer deaths (Zhou et al., 2020). Approximately 85% of lung cancer events are non-small cell lung cancer (NSCLC) (Wu et al., 2020). Currently, all kinds of various of strategies, specially the chemotherapy technique, are applied in lung cancer diagnosis and treatment (https://pubmed.ncbi.nlm.nih.gov/?term=Mart%20C3%ADn-S%20C3%A1nchez+JC&cauthor_id=30068667Liang+et+al.,+2019). The well-known chemotherapeutic agents, containing paclitaxel (https://pubmed.ncbi.nlm.nih.gov/?term=Mart%20C3%ADn-S%20C3%A1nchez+JC&cauthor_id=30068667Zhang+et+al.,+2020), cisplatin (https://pubmed.ncbi.nlm.nih.gov/?term=Mart%20C3%ADn-S%20C3%A1nchez+JC&cauthor_id=30068667Zhu+et+al.,+2020) and gemcitabine (https://pubmed.ncbi.nlm.nih.gov/?term=Mart%20C3%ADn-S%20C3%A1nchez+JC&cauthor_id=30068667Cao+et+al.,+2020), are used in lung cancer therapy. Whereas, patients with NSCLC had a poor prognosis, which attributed to the resistance of cancer cells to

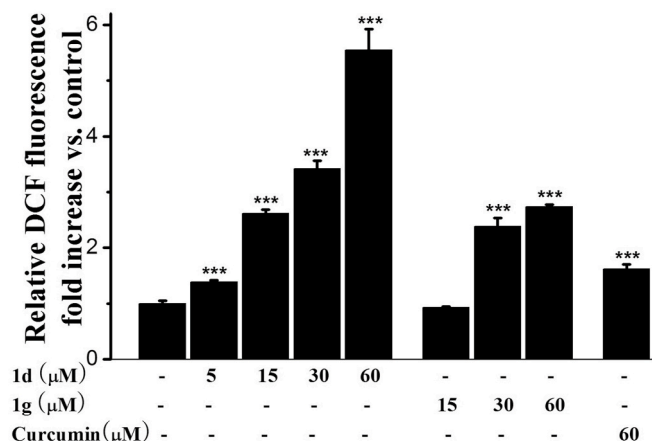


Fig. 3. The reactive oxygen species generation induced by curcumin and bischalcone analogs (1d and 1g) at the indicated concentrations on A549 cells. * $P < 0.05$, ** $P < 0.01$, *** $P < 0.001$ compared with control.

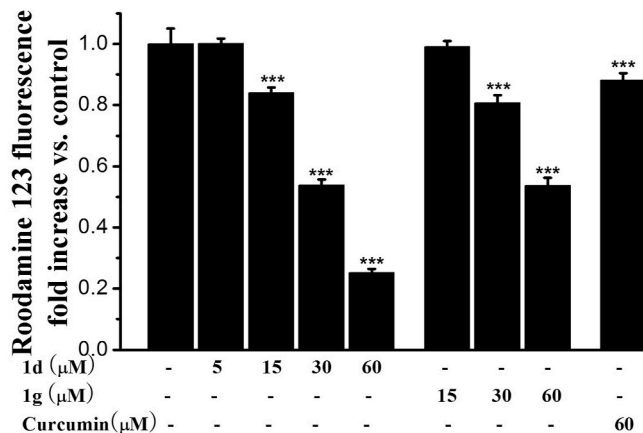


Fig. 6. Effects of curcumin and bischalcone analogs (1d and 1g) on the loss of mitochondrial membrane potential at the indicated concentrations in A549 cells for 12 h * $P < 0.05$, ** $P < 0.01$, *** $P < 0.001$ compared with control.

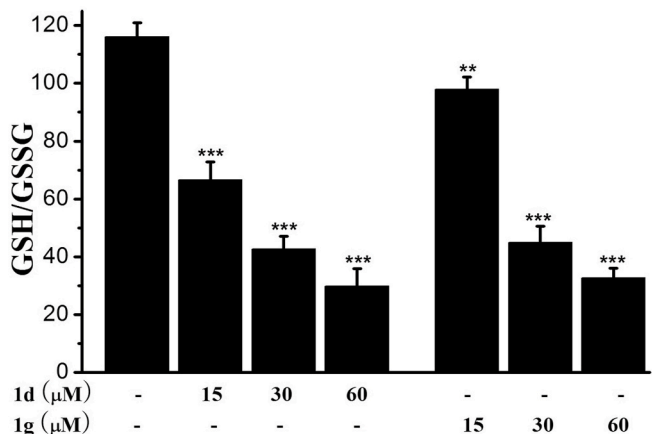


Fig. 4. The changes of GSH/GSSG ratios in A549 cells after treatment with 1d at the indicated concentrations for 6 h. Each experiment was performed in triplicate. * $P < 0.05$, ** $P < 0.01$, *** $P < 0.001$ compared with control.

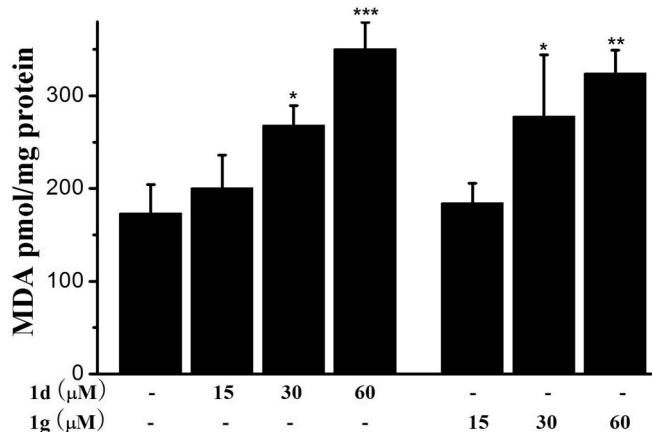


Fig. 5. The effects of bischalcone analogs (1d and 1g) at the indicated concentrations on the lipid peroxidation of A549 cells. Values are expressed as MDA equivalents (pmol)/mg protein. Each experiment was performed in triplicate. * $P < 0.05$, ** $P < 0.01$, *** $P < 0.001$ compared with control.

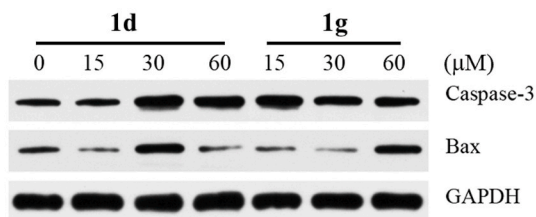


Fig. 7. The expression levels of Bax and Caspase 3 proteins in A549 cells promoted by bischalcone analogs 1d and 1g.

chemotherapy and metastasis (Ashrafizadeh et al., 2020). Extensive efforts need to be done to discovery new potential and impactful agents to fight against this disease.

Natural products have contributed notably to antitumor agents and it is estimated that most of the antitumor agents are of natural origin or inspired by natural compounds-. Curcumin, the naturally active ingredient found in turmeric, could affect various molecular pathway, such as nuclear factor-κB (NF-κB) (Liu et al., 2019), vascular endothelial growth factors (Qin et al., 2020) and PI3/Akt (Song et al., 2020) in treatment of lung cancer. Curcumin can induce apoptosis to reduce the viability and proliferation of lung cancer cells (Chen et al., 2020). Our previous work also illustrated that curcumin and its analogs could induce apoptosis by enhancing reactive oxygen species production in lung cancer (Liu et al., 2016). Bischalcones, the curcumin analogs with omitting the active methylene group, are promising candidates as these are important intermediates and raw materials widely used as precursors to drugs (Sharma et al., 2018). Curcumin-inspired bischalcone could accelerate cancer cell death through the inhibition of ATP-binding cassette superfamily G member 2 (ABCG2) protein (Winter et al., 2014) and promoting endoplasmic reticulum stress (Sansalone et al., 2019).

In this text, our data found that the bischalcone analogs 1d and 1g, the fluorine or methoxyl attached to the *ortho*-position of the aromatic ring(s), showed more potent cytotoxicity than that of curcumin and other bischalcone analogs (Table 1). This phenomenon may be attributed to the “*ortho effect*” of substituents (https://pubmed.ncbi.nlm.nih.gov/?term=Mart%3C%ADn-S%3C%3%A1nchez+JC&cauthor_id=30068667Dai+et+al.,+2015). Previously, the *ortho* hydroxyl group was affirmed to enhance remarkably the antiproliferation activity of cinnamaldehyde (https://pubmed.ncbi.nlm.nih.gov/?term=Mart%3C%ADn-S%3C%3%A1nchez+JC&cauthor_id=30068667Chew+et+al.,+2010) and chalcones (https://pubmed.ncbi.nlm.nih.gov/?term=Mart%3C%ADn-S%3C%3%A1nchez+JC&cauthor_id=30068667Gan+et+al.,+2013). Our previous work also proven that the *ortho* trifluoromethyl

([https://pubmed.ncbi.nlm.nih.gov/?term=Mart%C3%ADn-S%C3%A1nchez+JC&cauthor_id=30068667Dai et al., 2015](https://pubmed.ncbi.nlm.nih.gov/?term=Mart%C3%ADn-S%C3%A1nchez+JC&cauthor_id=30068667Dai+et+al.,+2015)) and *ortho* fluorine group ([https://pubmed.ncbi.nlm.nih.gov/?term=Mart%C3%ADn-S%C3%A1nchez+JC&cauthor_id=30068667Liu et al., 2016](https://pubmed.ncbi.nlm.nih.gov/?term=Mart%C3%ADn-S%C3%A1nchez+JC&cauthor_id=30068667Liu+et+al.,+2016)) could strengthen the cytotoxicity of mono-carbonyl curcumin analogs. Introduction of *ortho* groups may reveal a conformational change of a ligand by stereoelectronic effects, to impel its binding with the redox-sensitive target proteins ([https://pubmed.ncbi.nlm.nih.gov/?term=Mart%C3%ADn-S%C3%A1nchez+JC&cauthor_id=30068667Dai et al., 2015](https://pubmed.ncbi.nlm.nih.gov/?term=Mart%C3%ADn-S%C3%A1nchez+JC&cauthor_id=30068667Dai+et+al.,+2015)). The stereoelectronic effects could be proclaimed by calculating the geometries of **1d** and **1g** in the lowest energy conformation using Gaussian g09 program. Other factors including stabilities and cellular uptake of **1d** and **1g** should devote their cytotoxicity. Our results exhibited that compounds **1d** and **1g** showed the more stabilities than curcumin in RPMI 1640 supplemented with 10% (v/v) heat-inactivated fetal calf serum (Fig. 1). Curcumin analogs possessing “*ortho effect*” of substituents showed excellent cellular uptake in lung cancer in our previous work ([https://pubmed.ncbi.nlm.nih.gov/?term=Mart%C3%ADn-S%C3%A1nchez+JC&cauthor_id=30068667Liu et al., 2016](https://pubmed.ncbi.nlm.nih.gov/?term=Mart%C3%ADn-S%C3%A1nchez+JC&cauthor_id=30068667Liu+et+al.,+2016)).

Apoptosis, a common cell death pathway in chemotherapeutic agent, play a potent role in the development and maintenance of tissue homeostasis ([https://pubmed.ncbi.nlm.nih.gov/?term=Mart%C3%ADn-S%C3%A1nchez+JC&cauthor_id=30068667Benedetti et al., 2018](https://pubmed.ncbi.nlm.nih.gov/?term=Mart%C3%ADn-S%C3%A1nchez+JC&cauthor_id=30068667Benedetti+et+al.,+2018)). This study found that compounds **1d** and **1g** exhibited significant apoptosis of A549 cells with 66.4% and 52.4% late apoptotic cells, respectively. Increasing evidence has supported that reactive oxygen species overproduction, as an upstream apoptotic factor, is associated with apoptotic cell death (Pelicano et al., 2004). This study has shown that reactive oxygen species levels increased with an excellent dose-dependent manner induced by compounds **1d** and **1g** ($P < 0.01$, Fig. 3). The reactive oxygen species generation by curcumin analogs may be due to its ability to covalently modify TrxR (Fang et al., 2005). Compounds **1d** and **1g** could irreversibly inhibit TrxR and the modified enzyme converted into a prooxidant that triggered reactive oxygen species generation by an acquired NADPH oxidase.

A sustained higher reactive oxygen species production could result in the intracellular redox imbalance. This study indicated that the ratios of GSH/GSSG were present as an outstanding dose-dependent fashion after treatment with compounds **1d** and **1g**. The result was consistent with the reactive oxygen species generation abilities of **1d** and **1g**. Compounds **1d** and **1g** will go a step further to result in lipid peroxidation and the loss of mitochondrial membrane potential with an excellent dose-dependent manner. Moreover, **1d** and **1g** could increase the expression of Bax and Caspase 3 proteins, which play potential roles in the initiation and execution of apoptosis (Boice). The mechanisms of bischalcone-mediated apoptosis in A549 cells are still not fully clarified. The stereoelectronic effects of bischalcones and the specific mechanism of reactive oxygen species and apoptosis still requires further research.

5. Conclusions

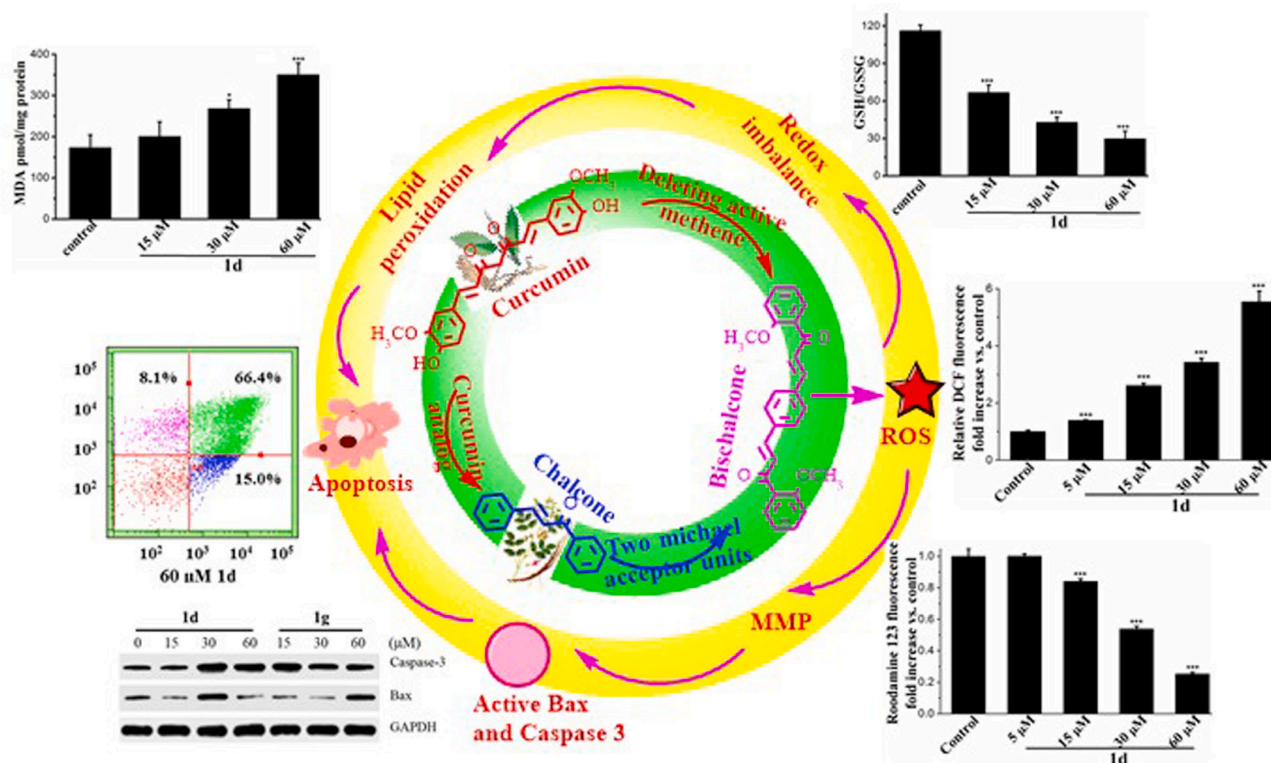
In conclusion, we had synthesized a panel of bischalcone analogs through the Aldol condensation reaction, and confirmed their structures by the ^1H NMR and ^{13}C NMR. Then, we found that **1d** and **1g** exhibited more potent cytotoxicity against A549 cells than curcumin and other bischalcone analogs. Furthermore, the results indicated that reactive oxygen species exerted a key role in **1d** and **1g**-triggered apoptosis and act as an upstream signal to regulate the redox balance, lipid peroxidation, the disruption of MMP, the expression levels of Bax and Caspase 3 (Scheme 2). Therefore, the present study supported that enhancing the reactive oxygen species production may be a potential strategy to improve the anticancer activity of bischalcone analogs.

Ethics approval and consent to participate

No human or animal related experiments in the present study.

Consent for publication

All authors give the consent for the publish of this study.



Scheme 2. **1d** induce reactive oxygen species-Mediated apoptosis in A549 cells.

Availability of data and material

Data made available to all interested researchers upon request.

CRediT authorship contribution statement

Jie Yang: Methodology, Formal analysis, Investigation, Resources, Data curation, Writing - original draft, Writing - review & editing, Funding acquisition. **Wen-Wen Mu:** Methodology, Formal analysis, Investigation, Resources, Data curation. **Guo-Yun Liu:** Writing - original draft, Writing - review & editing, Supervision, Project administration, Funding acquisition.

Declaration of competing interest

The authors declare that they have no conflict of interest.

Acknowledgements

This work was supported by the National Natural Science Foundation of China (Grant No. 81901420), Shandong Provincial Natural Science Foundation (Grant No. ZR2018LH022), the Open Project of Shandong Collaborative Innovation Centre for Antibody Drugs (Grant No. CIC-AD1822 and CIC-AD1824).

Appendix A. Supplementary data

Supplementary data to this article can be found online at <https://doi.org/10.1016/j.ejphar.2020.173396>.

References

- Ashrafzadeh, M., Najafi, M., Makvandi, P., Zarrabi, A., Farkhondeh, T., Samarghandian, S., 2020. Versatile role of curcumin and its derivatives in lung cancer therapy. *J. Cell. Physiol.* 1–28 <https://doi.org/10.1002/jcp.29819>.
- Benedetti, S., Catalani, S., Palma, F., Canonico, B., Luchetti, F., Galati, R., Papa, S., Battistelli, S., 2018. Acyclovir induces cell cycle perturbation and apoptosis in jurkat leukemia cells, and enhances chemotherapeutic drug cytotoxicity. *Life Sci.* 215, 80–85. <https://doi.org/10.1016/j.lfs.2018.11.002>.
- Cao, W.J., Yang, Q., Yuan, Z.J., Li, H., Wang, W.W., Xiao, X.J., Wang, Z., Liang, L., Zhou, P., Liu, J., Hu, X.M., Zhang, B., 2020. Gemcitabine inhibits cisplatin resistance in cisplatin-resistant A549 cells by upregulating trx-interacting protein and inducing cell cycle arrest. *Biochem. Biophys. Res. Commun.* 524, 549–554. <https://doi.org/10.1016/j.bbrc.2020.01.130>.
- Chen, T.K., Zhao, L.Q., Chen, S.N., Zheng, B., Chen, H., Zeng, T.N., Sun, H.X., Zhong, S.J., Wu, W.C., Lin, X.K., Wang, L.H., 2020. The curcumin analogue WZ35 affects glycolysis inhibition of gastric cancer cells through ROS-YAP-JNK pathway. *Food Chem. Toxicol.* 137 <https://doi.org/10.1016/j.fct.2020.111131>, 111131.
- Chew, E.H., Nagle, A.A., Zhang, Y., Scarmagnani, S., Palaniappan, P., Bradshaw, T.D., Holmgren, A., Westwell, A.D., 2010. Cinnamaldehydes inhibit thioredoxin reductase and induce Nrf2: potential candidates for cancer therapy and chemoprevention. *Free Radic. Biol. Med.* 48, 98–111. <https://doi.org/10.1016/j.freeradbiomed.2009.10.028>.
- Dai, F., Liu, G.Y., Li, Y., Yan, W.J., Wang, Q., Yang, J., Lu, D.L., Lin, D., Zhou, B., 2015. Insights into the importance for designing curcumin-inspired anticancer agents by a prooxidant strategy: the case of diarylpentanooids. *Free Radic. Biol. Med.* 85, 127–137. <https://doi.org/10.1016/j.freeradbiomed.2015.04.017>.
- Fang, J.G., Lu, J., Holmgren, A., 2005. Thioredoxin reductase is irreversibly modified by curcumin a novel molecular mechanism for its anticancer activity. *J. Biol. Chem.* 280, 25284–25290. <https://doi.org/10.1074/jbc.m414645200>.
- Gan, F.F., Kaminska, K.K., Yang, H., Liew, C.Y., Leow, P.C., So, C.L., Tu, L.N., Roy, A., Yap, C.W., Kang, T.S., 2013. Identification of Michael acceptor-centric pharmacophores with substituents that yield strong thioredoxin reductase inhibitory character correlated to antiproliferative activity. *Antioxidants Redox Signal.* 19, 1149–1165. <https://doi.org/10.1089/ars.2012.4909>.
- Liang, X.J., Guan, Y.P., Zhang, B.C., Liang, J., Wang, B.C., Li, Y., Wang, J., 2019. Severe immune-related pneumonitis with PD-1 inhibitor after progression on previous PD-L1 inhibitor in small cell lung cancer: a case report and review of literature. *Front Oncol* 9, 1437. <https://doi.org/10.3389/fonc.2019.01437>.
- Liu, G.Y., Zhai, Q., Chen, J.Z., Zhang, Z.Q., Yang, J., 2016. 2,2'-Fluorine mono-carbonyl curcumin induce reactive oxygen species-Mediated apoptosis in Human lung cancer NCI-H460 cells. *Eur. J. Pharmacol.* 786, 161–168. <https://doi.org/10.1016/j.ejphar.2016.06.009>.
- Liu, G.Y., Jia, C.C., Han, P.R., Yang, J., 2018. 3,5-Bis(2-fluorobenzylidene)-4-piperidone induce reactive oxygen species-mediated apoptosis in A549 cells. *Med. Chem. Res.* 27, 128–136. <https://doi.org/10.1007/s00044-017-2056-x>.
- Liu, J.B., Hu, L., Yang, Z.J., Sun, Y., Hoffman, R.M., Yi, Z., 2019. Aurora-A/NF-κB signaling is associated with radio-resistance in human lung adenocarcinoma. *Anticancer Res.* 3911, 5991–5998. <https://doi.org/10.21873/anticancer.13804>.
- Ma, Y.Y., Di, Z.M., Cao, Q., Xu, W.S., Bi, S.X., Yu, J.S., Shen, Y.J., Yu, Y.Q., Shen, Y.X., Feng, L.J., 2020. Xanthatin induces glioma cell apoptosis and inhibits tumor growth via activating endoplasmic reticulum stress-dependent CHOP pathway. *Acta Pharmacol. Sin.* 41, 404–414. <https://doi.org/10.1038/s41401-019-0318-5>.
- Malvezzi, M., Carioli, G., Bertuccio, P., Boffetta, P., Levi, F., La Vecchia, C., Negri, E., 2019. European cancer mortality predictions for the year 2019 with focus on breast cancer. *Ann. Oncol.* 30, 781–787. <https://doi.org/10.1093/annonc/mdz051>.
- Martín-Sánchez, J.C., Lunet, N., González-Marrón, A., Lidón-Moyano, C., Matilla-Santander, N., Cléries, R., Malvezzi, M., Morais, S., Costa, A.R., Ferro, A., Lopes-Conceicao, L., La Vecchia, C., Martínez-Sánchez, J.M., 2018. Projections in breast and lung cancer mortality among women: a bayesian analysis of 52 countries worldwide. *Canc. Res.* 78, 4436–4442. <https://doi.org/10.1158/0008-5472.CAN-18-0187>.
- Mu, W.W., Cao, Y.X., Tie, X.R., Li, T., Zhu, Z.Z., Yang, J., Liu, G.Y., 2020. Fluorinated mono-carbonyl curcumin analogues induce reactive oxygen species to enhance apoptosis in human colon cancer HCT116 cells. *Lat. Am. J. Pharm.* 39, 361–365.
- Pelicano, H., Carney, D., Huang, P., 2004. ROS stress in cancer cells and therapeutic implications. *Drug Resist. Updates* 7, 97–110. <https://doi.org/10.1016/j.drup.2004.01.004>.
- Qin, L.M., Zhong, M.L., Adah, D., Qin, L., Chen, X.P., Ma, C.Q., Fu, Q., Zhu, X.P., Li, Z.L., Wang, N.N., Chen, Y.F., 2020. A novel tumour suppressor lncRNA F630028O10Rik inhibits lung cancer angiogenesis by regulating miR-223-3p. *J. Cell Mol. Med.* 24, 3549–3559. <https://doi.org/10.1111/jcmm.15044>.
- Reddy, M.V.B., Shen, Y., Ohkoshi, E., Bastow, K.F., Lee, K., Wu, T., 2012. Bis-chalcone analogues as potent NO production inhibitors and as cytotoxic agents. *Eur. J. Med. Chem.* 47, 97–103. <https://doi.org/10.1016/j.ejmech.2011.10.026>.
- Sansalone, L., Veliz, E.A., Myrthil, N., Stathias, V., Walters, W., Torrens, I.I., Schürer, S. C., Vanni, S., Leblanc, R.M., Graham, R.M., 2019. Novel curcumin inspired bis-chalcone promotes endoplasmic reticulum stress and glioblastoma neurosphere cell death, 11, p. 357. <https://doi.org/10.3390/cancers11030357>.
- Santos, C.C.F., Paradelo, L.S., Novaes, L.F.T., Dias, S.M.G., Pastre, J.C., 2017. Design and synthesis of cenoclidamide analogues and their evaluation against breast cancer cell lines. *MedChemComm* 8, 755–766. <https://doi.org/10.1039/c6md00577b>.
- Serrano, J.J., Delgado, B., Medina, M.A., 2020. Control of tumor angiogenesis and metastasis through modulation of cell redox state. *BBA-Reviews on Cancer.* <https://doi.org/10.1016/j.bbcan.2020.188352>, 1873, 188352.
- Sharma, U.K., Mohanakrishnan, D., Sharma, N., Equbal, D., Sahal, D., Sinha, A.K., 2018. Facile synthesis of vanillin-based novel bischalcones identifies one that induces apoptosis and displays synergy with Artemisinin in killing chloroquine resistant Plasmodium falciparum, 155, pp. 623–638. <https://doi.org/10.1016/j.ejmech.2018.06.025>.
- Song, Y.X., Zhou, B., Du, X.Y., Wang, Y., Zhang, J., Ai, Y.Q., Xia, Z.J., Zhao, G.F., 2020. Folic acid (FA)-conjugated mesoporous silica nanoparticles combined with MRP-1 siRNA improves the suppressive effects of myricetin on non-small cell lung cancer (NSCLC). *Biomed. Pharmacother.* 125 <https://doi.org/10.1016/j.biopha.2019.109561>, 109561.
- Wang, Y., Chen, X.Y., Li, Y., Wang, Y., Xu, F., 2019. An orally antitumor chalcone hybrid inhibited HepG2 cells growth and migration as the tubulin binding agent. *Invest. N. Drugs* 37, 784–790. <https://doi.org/10.1007/s10637-019-00737-z>.
- Winter, E., Neuenfeldt, P.D., Chiaradia-Delatorre, L.D., Gauthier, C., Yunes, R.A., Nunes, R.J., Creczynski-Pasa, T.B., Pietro, A.D., 2014. Symmetric bis-chalcone as a new type of breast cancer resistance protein inhibitors with a mechanism different from that of chromones. *J. Med. Chem.* 57, 2930–2941. <https://doi.org/10.1021/jm401879z>.
- Wu, Y.Z., Si, Y., Xiang, Y.C., Zhou, T., Liu, X.W., Wu, M.W., Li, W.J., Zhang, T., Xiang, K., Zhang, L., Zhao, H.Z., Liu, Y., 2020. Polyphyllin I activates AMPK to suppress the growth of non-small-cell lung cancer via induction of autophagy. *Arch. Biochem. Biophys.* 687 <https://doi.org/10.1016/j.abb.2020.108285>, 108285.
- Yang, J., Li, J., Qu, X.Y., Liu, G.Y., Liu, R.M., 2019. A novel resveratrol derivative induces oxidative stress, G1 cell cycle arrest and premature senescence in A549 cells. *Lat. Am. J. Pharm.* 38, 907–917.
- Zhang, H.L., Ren, X.L., Yang, W.H., Xie, Y., Yang, J., Liu, G.Y., Guo, S.J., 2018. Synthesis and evaluation of anti-cancer activities of mono-carbonyl curcumin analogs. *Lat. Am. J. Pharm.* 37, 958–963.
- Zhang, L.X., Wang, X.W., Cueto, R., Effi, C., Zhang, Y.L., Tan, H.M., Qin, X.B., Ji, Y., Yang, X.F., Wang, H., 2019. Biochemical basis and metabolic interplay of redox regulation. *Redox Bio* 26. <https://doi.org/10.1016/j.redox.2019.101284>, 101284.
- Zhang, M., Li, M., Du, L., Zeng, J., Yao, T., Jin, Y., 2020. Paclitaxel-in-liposome-in-bacteria for inhalation treatment of primary lung cancer. *International Journal of Pharmaceutics* 578. <https://doi.org/10.1016/j.ijpharm.2020.119177>, 119177.
- Zhou, W.L., Liu, Y.Q., Gao, Y., Cheng, Y.D., Chang, R.M., Li, X.Z., Zhou, Y.W., Wang, S. Q., Liang, L.B., Duan, C.J., Zhang, C.F., 2020. MICAL2 is a novel nucleocytoplasmic shuttling protein promoting cancer invasion and growth of lung adenocarcinoma. *Canc. Lett.* 483, 75–86. <https://doi.org/10.1016/j.canlet.2020.04.019>.
- Zhu, H., Yang, J., Yang, S., 2020. MicroRNA-103a-3p potentiates chemoresistance to cisplatin in non-small cell lung carcinoma by targeting neurofibromatosis 1. *Exp. Ther. Med.* 19, 1797–1805. <https://doi.org/10.3892/etm.2020.8418>.